

Published in final edited form as:

Nat Immunol. 2008 August ; 9(8): 857–865. doi:10.1038/ni.1636.

The NALP3 inflammasome is involved in the innate immune response to amyloid- β

Annett Halle¹, Veit Hornung¹, Gabor C Petzold², Cameron R Stewart³, Brian G Monks¹, Thomas Reinheckel⁴, Katherine A Fitzgerald¹, Eicke Latz¹, Kathryn J Moore³, and Douglas T Golenbock¹

¹Department of Infectious Diseases and Immunology, University of Massachusetts Medical School, Worcester, Massachusetts 01605, USA

²Center for Brain Science and Department of Molecular and Cellular Biology, Harvard University, Cambridge, Massachusetts 02138, USA

³Lipid Metabolism Unit, Massachusetts General Hospital, Harvard Medical School, Boston, Massachusetts 02114, USA

⁴Institute for Molecular Medicine und Cell Research, Albert-Ludwigs University, Freiburg 79104, Germany

Abstract

The fibrillar peptide amyloid- β (A β) has a chief function in the pathogenesis of Alzheimer's disease. Interleukin 1 β (IL-1 β) is a key cytokine in the inflammatory response to A β . Insoluble materials such as crystals activate the inflammasome formed by the cytoplasmic receptor NALP3, which results in the release of IL-1 β . Here we identify the NALP3 inflammasome as a sensor of A β in a process involving the phagocytosis of A β and subsequent lysosomal damage and release of cathepsin B. Furthermore, the IL-1 β pathway was essential for the microglial synthesis of proinflammatory and neurotoxic factors, and the inflammasome, caspase-1 and IL-1 β were critical for the recruitment of microglia to exogenous A β in the brain. Our findings suggest that activation of the NALP3 inflammasome is important for inflammation and tissue damage in Alzheimer's disease.

Alzheimer's disease is a devastating neurodegenerative disease characterized by widespread neuronal cell death and progressive dementia. It is widely accepted that the extracellular accumulation of amyloid- β (A β) in senile plaques is a principal event in the pathogenesis of Alzheimer's disease^{1,2}, but the cellular events leading to plaque-induced neuronal dysfunction have remained less clear. Studies have suggested that inflammatory and immunological processes are not mere bystanders but that microglia and invading bone marrow-derived mononuclear phagocytes are central to the initiation and progression of Alzheimer's disease^{1,3}. Microglia are activated by and recruited to senile plaques², phagocytose A β ³, and secrete cytokines after activation⁴. Moreover, systemic inhibition of inflammation or immunization against A β decreases plaque burden and delays disease onset, which indicates that pharmacological intervention in immunological pathways may potentially hold great therapeutic promise^{1,5,6}. Despite the central function attributed to the immune system in Alzheimer's disease, the initiating signaling pathways that ultimately lead

© 2008 Nature Publishing Group

Correspondence should be addressed to D.T.G. (douglas.golenbock@umassmed.edu).

Accession codes. UCSD-Nature Signaling Gateway (<http://www.signaling-gateway.org>): A003663 and A000492.

Note: Supplementary information is available on the Nature Immunology website.

to the activation and recruitment of microglia and macrophages are not completely understood.

One prominent and early cytokine consistently found in diseased tissues is interleukin 1 β (IL-1 β ; A003663). IL-1 β is released by activated microglia after stimulation with A β *in vitro*⁷, and higher expression of IL-1 β has been detected in microglia cells surrounding A β plaques in patients with Alzheimer's disease and in animal models of this disease^{3,8}. Furthermore, higher concentrations of IL-1 β have been detected in the cerebrospinal fluid of patients with this disease⁹. However, the mechanisms by which A β mediates IL-1 β release are poorly understood.

IL-1 β is produced as the inactive precursor pro-IL-1 β in the cytosol after cellular activation by a variety of stimuli¹⁰. The protease caspase-1 (A000492) is critically involved in inflammatory responses because of its pivotal function in regulating the cleavage and maturation of pro-IL-1 β . The activity of caspase-1 is tightly controlled by cytosolic multiprotein complexes called 'inflammasomes'. The cytoplasmic receptors of the NALP family are central components of the inflammasome that associate with the adaptor protein ASC, which in turn recruits proinflammatory caspase precursors such as pro-caspase-1. Inflammasomes containing NALP3 can be activated by bacterial toxins, as well as by endogenous 'danger' signals such as urate crystals^{11,12}.

Here we found that the NALP3 inflammasome was required for the A β -induced activation of caspase-1, the release of mature IL-1 β and the secretion of proinflammatory and potentially neurotoxic cytokines and chemokines. Activation of the NALP3 inflammasome was initiated after A β phagocytosis and subsequent lysosomal damage in a process that partially involved the lysosomal protease cathepsin B. Our findings indicate that activation of the NALP3 inflammasome by A β may represent a critical component of the inflammatory response in Alzheimer's disease.

RESULTS

Fibrillar A β induces IL-1 β from microglia

Activated microglia in senile plaques have high expression of IL-1 β ⁸, and higher concentrations of IL-1 β are found in the cerebrospinal fluid of patients with Alzheimer's disease⁹. To investigate the mechanisms of the A β -triggered maturation and release of IL-1 β *in vitro*, we incubated primary mouse microglial cells with fibrillar A β and its reverse form, nonfibrillar A β (revA β). Because pro-IL-1 β is not constitutively expressed and requires transcriptional induction, we primed cells with lipopolysaccharide (LPS), as in published studies¹¹⁻¹³, to ensure robust induction of pro-IL-1 β and to mimic the chronic activation of microglia in the plaque-bearing brain²⁻⁴.

We found that fibrillar A β but not revA β led to early and notable release of IL-1 β into the supernatants (Fig. 1a). We found a similar rate of IL-1 β release in a mouse microglial cell line that we established from wild-type C57/BL6 mice (Fig. 1b). These immortalized microglial cell lines were similar to primary mouse microglial preparations in morphology, expression of cell surface markers and function (Supplementary Fig. 1a,b online).

IL-1 β maturation is controlled by caspase-1 after assembly of the inflammasome, which activates pro-caspase-1. To test whether A β activates caspase-1, we measured activated caspase-1 with a fluorescent cell-permeable probe that covalently binds only to activated caspase-1 (ref. 14). This reagent did not lead to any visible staining in caspase-1-deficient cells (data not shown). Confocal microscopy as well as flow cytometry showed a robust increase in caspase-1-positive microglial cells after stimulation with A β , as well as after

stimulation with the NALP3 inflammasome activator ATP, whereas cells stimulated with revA β showed no such response (Fig. 1c). We obtained similar results with primary microglial cultures (Supplementary Fig. 1c).

Furthermore, immunoblot analysis of caspase-1 showed that A β induced cleavage of caspase-1 (to its active p10 subunit) at a concentration of 10 μ M, as did the positive controls ATP and transfected double-stranded DNA (poly(dA:dT)), whereas revA β at the same concentration initiated no specific cleavage of caspase-1 (Fig. 1d). Finally, we noted dose-dependent inhibition of IL-1 β release when we stimulated wild-type immortalized microglial cells with A β in the presence of a caspase-1-specific inhibitor (Fig. 1e). We also noted this effect in primary microglia (Supplementary Fig. 1d). These data collectively indicate that the A β -induced release of IL-1 β from microglia is mediated by activated caspase-1.

Fibrillar A β activates the NALP3 inflammasome

Next we sought to determine the pathway responsible for caspase-1 activation and subsequent IL-1 β release. Specifically, we investigated whether the NALP3 inflammasome and ASC, the inflammasome adaptor protein involved in the autocatalysis of pro-caspase-1 (ref. 15), were required. First we stably transduced microglial cell cultures with a fusion protein of ASC and cyan fluorescent protein (CFP-ASC). ASC forms large oligomers after its activation, which leads to visible changes in the cytoplasmic fluorescence pattern of CFP-ASC. The clustering of CFP-ASC can be used as an 'optical reporter' of ASC activation¹⁶. We found that in baseline conditions, CFP-ASC fluorescence was evenly distributed in the cytoplasm and nucleus (Fig. 2a). At 3 h after stimulation with A β , brightly fluorescent clusters of CFP-ASC formed in the cytoplasm of many cells; we also noted these clusters after stimulation with ATP but not with revA β or LPS alone (Fig. 2a,b), which indicated that they represent cytoplasmic aggregates of activated ASC.

To investigate whether A β specifically activates the NALP3 inflammasome, we used bone marrow-derived macrophages from mice deficient in NALP3 or ASC. We noted strong and dose-dependent release of IL-1 β by macrophages from wild-type mice, whereas macrophages from mice deficient in NALP3 or ASC failed to release IL-1 β after stimulation with A β (Fig. 2c). These results show that A β activates the NALP3 inflammasome, resulting in caspase-1 activation and subsequent maturation and release of IL-1 β .

A β causes lysosomal damage and IL-1 β release

We next explored the mechanism by which A β activates the NALP3 inflammasome. The NALP3 inflammasome is known to be activated by bacterial toxins, and several crystals and their phagocytosis have been shown to be important for activation of the NALP3 inflammasome¹³. Microglia are known to phagocytose A β *in vitro* and *in vivo*³. We therefore investigated whether phagocytosis was required for the A β -induced release of IL-1 β . We incubated microglial cells with cytochalasin D, an inhibitor of the phagocytosis of A β ¹⁷, before and during stimulation with A β . We found that the A β -induced release of IL-1 β from microglia was attenuated by cytochalasin D (Fig. 3a), which indicated that phagocytosis is required for the induction of IL-1 β by A β . Cytochalasin D had no effect on the release of IL-1 β after stimulation with ATP (Fig. 3a).

Next we investigated phagocytosis of A β labeled with fluorescein isothiocyanate (FITC). Immunocytochemistry showed that after 3 h, most FITC-labeled A β was internalized by microglia into discrete, large, intracellular compartments (Fig. 3b, top). We identified these as lysosomes, as their membranes stained positively for the lysosomal marker protein LAMP-1 (Fig. 3b, bottom). Confocal *z*-series analysis showed that in many cells (about 15% of all cells), A β -containing lysosomes were extensively enlarged and swollen (Fig. 3c). We

noted A β -containing lysosomes of up to 11 μm in diameter ($4.1 \pm 0.4 \mu\text{m}$ (mean \pm s.e.m.)) that were much larger than intact microglial lysosomes ($1.1 \pm 0.05 \mu\text{m}$ on average; Fig. 3d). These results show that A β is rapidly phagocytosed by microglia and that lysosomal swelling, and possible dysfunction, occurs during the internalization.

To further explore whether lysosomal damage occurs during the phagocytosis of A β , we simultaneously monitored lysosomal integrity and phagocytosis of fluorescence-labeled A β by confocal microscopy. We identified intact lysosomes by their accumulation of a lysosome-specific ('lysomotropic') dye that is fluorescent at acidic pH. Live confocal microscopy showed that lysosomes positive for this dye rapidly accumulated fibrillar A β (Fig. 3e). Shortly after incubation with A β , lysosomal size increased (Fig. 3d), as described above. However, these enlarged lysosomes, although readily identifiable by their accumulation of A β and by contrast interference imaging, did not show enrichment for the lysomotropic dye (Fig. 3e), which indicated that acidification and function were compromised in enlarged A β -containing lysosomes. Consistent with that visual analysis, quantification of accumulation of the dye in microglial cultures by flow cytometry showed that with increasing amounts of A β , the percentage of cells that were negative for fluorescence increased in a dose-dependent way (Fig. 3f). These data indicate that A β leads to lysosomal swelling, destabilization and dysfunction.

Lysosomal damage triggers release of cathepsin B

We next explored the possibility that the release of lysosomal factors into the cytosolic compartment, rather than direct actions of A β , might be responsible for the subsequent activation of the NALP3 inflammasome and caspase-1. Lysosomes contain many proteolytic enzymes, including those of the cathepsin family. Cathepsin B, one of its members, has been linked before to the pathogenesis of Alzheimer's disease. Larger amounts of cathepsin B have been reported in microglia surrounding senile plaques¹⁸, and inhibition of cathepsin B has proven therapeutically beneficial in a mouse model of Alzheimer's disease¹⁹. We therefore investigated whether cathepsin B was released after A β -induced lysosomal damage in microglia. Using an antibody to cathepsin B, we found that in unstimulated cells, intracellular cathepsin B had the expected punctuated staining pattern, consistent with its localization in lysosomes (Fig. 4a, left). Early after phagocytosis of FITC-labeled A β , cathepsin B localized together with A β in small, structurally intact lysosomes (Fig. 4a, middle). However, at 4 h after A β stimulation, the lysosomes of 15–20% of cells were enlarged and did not stain for cathepsin B (Fig. 4a, right). Notably, the overall cellular staining pattern of cathepsin B seemed diffuse and less punctuate (Fig. 4a, right) and was outside LAMP-1-positive enlarged lysosomes (Fig. 4a, far right), which indicated release of cathepsin B from damaged lysosomes into the cytoplasm.

To investigate whether the activity of cathepsin B after stimulation with A β was functionally linked to microglial activation, we measured the effect of the inhibition of cathepsin B on the release of IL-1 β from microglia. We found that a specific inhibitor of cathepsin B²⁰ inhibited microglial IL-1 β release in a dose-dependent way (Fig. 4b), whereas inhibitors of cathepsin D and cathepsin L had no effect (Fig. 4b). Moreover, all three cathepsin inhibitors at their highest concentration did not inhibit IL-1 β release when microglia were stimulated with ATP (Fig. 4b). Consistent with those findings, IL-1 β release was much lower in cathepsin B-deficient cells than in wild-type cells after stimulation with A β at various concentrations, whereas IL-1 β release was similarly high after stimulation with ATP or poly(dA:dT) in cathepsin B-deficient and wild-type cells (Fig. 4c). These data indicate that the effect of A β on IL-1 β release was specifically linked to cathepsin B and was not related to effects on general cell physiology.

To investigate whether the cathepsin B–induced release of IL-1 β occurred through activation of caspase-1 and not by caspase-1-independent mechanisms, we directly quantified caspase-1 activation in microglia with the fluorescent cell-permeable probe that covalently binds only to activated caspase-1 (used in Fig. 1c). Flow cytometry showed that caspase-1 activation after stimulation with A β was inhibited by the cathepsin B inhibitor in a dose-dependent way (Fig. 4d). The induction of caspase-1 activation was not affected by cathepsin B inhibition when cells were stimulated with ATP (Fig. 4d), which again emphasized the specific link between A β and cathepsin B. Overall, these results indicate that microglial phagocytosis of A β induces lysosomal enlargement and loss of lysosomal integrity, which leads to release of the lysosomal contents into the cytoplasm. Furthermore, the release of specific proteases seems to be causally related to inflammasome activation.

A β -induced proinflammatory and chemotactic factors

Microglia surrounding A β -containing senile plaques acquire an activated morphology and secrete chemotactic and proinflammatory molecules⁴, which contribute to the recruitment of microglia and may amplify the neurotoxic effects of A β . We sought to determine whether activation of caspase-1 was involved in the A β -induced secretion of these factors. First we studied the release of nitric oxide and TNF from microglia, as these are two important mediators of A β -induced neurotoxicity and inflammation^{21,22}. The synthesis of nitric oxide in immortalized microglial cultures was attenuated considerably in a dose-dependent way by inhibition of caspase-1 with a caspase-1-specific inhibitor (Fig. 5a). Furthermore, nitric oxide was not produced by microglial cultures from caspase-1-deficient mice after A β stimulation (Fig. 5b). Similarly, A β -induced release of TNF was attenuated by caspase-1 inhibition (Fig. 5c) and was absent from caspase-1-deficient microglia (Fig. 5d). To ensure that the attenuation of cytokine release by caspase-1 inhibition was related to actions of IL-1 β and not to IL-1 β -independent effects of caspase-1, we analyzed the production of nitric oxide and TNF in microglia deficient in IL-1 receptor (IL-1R). We found that the release of these factors was much lower in IL-1R-deficient microglia (Supplementary Fig. 2a,b online). Notably, IL-1 β remained unchanged relative to that in wild-type microglia cells (Supplementary Fig. 2c), which indicated that the production of nitric oxide and TNF depends on autocrine and paracrine effects of IL-1 β after caspase-1 activation and is unrelated to other effects of caspase-1. As a control, nitric oxide and TNF were equally high in both cell lines after stimulation with the inflammasome-independent activator zymosan (Supplementary Fig. 2a,b). These data show that the release of important neurotoxic and proinflammatory factors depends on the activation of caspase-1 and subsequent IL-1 signaling.

To confirm that ‘upstream’ activation of the NALP3 inflammasome was necessary for caspase-1-dependent production of those factors, we measured the release of nitric oxide by macrophage cells from NALP3-deficient and ASC-deficient mice. As controls, we used cells from wild-type mice and mice deficient in Ipaf, which is part of a different inflammasome typically activated by intracellular bacterial pathogens²³. Consistent with the central function of the NALP3 inflammasome in A β -induced activation of caspase-1, we did not detect much release of nitric oxide from cultures of macrophages from NALP3-deficient or ASC-deficient mice, whereas we measured considerable production of nitric oxide by cultures of cells from IPAF-deficient and wild-type mice (Fig. 5e). These data indicate that activation of the NALP3 inflammasome by A β is an important trigger for subsequent ‘downstream’ activation of inflammatory and potentially cytotoxic mediators.

We therefore directly investigated whether caspase-1 contributed to neuronal dysfunction *in vitro*. We incubated A β with a mouse neuronal cell line and found only minimal morphological and quantitative effects (Fig. 5f, left), as described before in a similar system²⁴. In contrast, in mixed neuronal cell–microglial cell cultures with wild-type

microglial cells, A β induced widespread neuronal cell death (Fig. 5f, middle), whereas we noted no neurotoxic effects of A β in mixed neuronal cell–microglial cell cultures with caspase-1-deficient microglia (Fig. 5f, right).

Microglia have been shown to upregulate and secrete mononuclear phagocyte chemoattractants in response to A β ²⁵; these contribute to the additional accumulation of microglial cells around senile plaques. To investigate if the caspase-1 pathway was also involved in the upregulation of chemotactic cytokines, we stimulated wild-type and caspase-1-deficient microglial cells with A β and measured the induction of mRNA encoding CCL3 (MIP-1 α), CCL4 (MIP-1 β) and CXCL2 (MIP-2) by real-time quantitative PCR. A β upregulated the expression of these chemokines in wild-type cells in a time-dependent way, as described before²⁵, whereas microglial cells deficient in caspase-1 failed to upregulate chemokine mRNA (Fig. 5g). These results collectively suggest that the NALP3 inflammasome, through activation of caspase-1, contributes to the proinflammatory, chemotactic and neurotoxic effects of A β mediated by microglia.

IL-1-mediated pathways contribute to microglial activation

Finally we investigated whether microglial chemotaxis and activation *in vivo* is mediated by inflammasome components, caspase-1 and the IL-1 pathway. For this, we stereotactically injected fibrillar A β into the striatum of anesthetized adult mice. This model has been used to study the inflammatory effects of A β *in vivo* and to investigate microglial function in models of Alzheimer's disease^{26,27}. As a control, we injected revA β into the contralateral hemisphere. Immunohistochemistry of fixed brain sections stained with an antibody to the microglial and macrophage marker F4/80 at 48 h after injection showed considerable recruitment and chemotaxis of microglia around the injection site, whereas only a few cells accumulated in the contralateral hemisphere injected with revA β (Fig. 6).

Next we used various knockout mouse lines to explore the function of the inflammasome, caspase-1 activation and IL-1 signaling in the recruitment of microglia to A β *in vivo* (Fig. 6). First we found that microglial recruitment and activation was much lower in mice deficient in the inflammasome component ASC. Similarly, mice deficient in caspase-1 also had only very attenuated microglial activation after A β injection. Finally, recruitment and accumulation of microglia to A β was much lower in mice deficient in the IL-1R or in the IL-1R adaptor protein MyD88. Microglial activation in the contralateral hemispheres injected with revA β was very low in all groups (Fig. 6). These data demonstrate that as with microglia *in vitro*, microglial activation *in vivo* is dependent on activation of the inflammasome and caspase-1 and subsequent initiation of the IL-1 pathway.

DISCUSSION

A variety of structurally diverse molecules, including ATP¹², imidazoquinoline derivatives²⁸, bacterial toxins¹² and various crystals^{11,13}, are known to activate the NALP3 inflammasome. Here we found that an endogenous peptide, A β , which forms insoluble fibrils in the brains of patients with Alzheimer's disease, activated the NALP3 inflammasome. A β therefore seems to constitute another very clinically relevant endogenous 'danger' signal that is sensed by the NALP3 inflammasome. Although additional examples of fibrillar endogenous peptides that activate this pathway remain to be identified, we suspect that A β represents the first of a class of aggregated proteins that may share similar actions. It is conceivable that the NALP3 inflammasome may function as a general sensor for the recognition of peptide or protein aggregates that are also involved in the pathogenesis of diseases such as Parkinson's and systemic amyloidosis and thus may be involved in inducing inflammatory responses in other disorders.

It has remained an open issue whether the NALP3 inflammasome is activated through direct binding to its ligands, similar to what has been described for Toll-like receptors²⁹, or through intermediary pathways that may be shared by different activators. A common structural finding among many different NALP3 activators is that they are of a particulate nature, and it thus seems possible that the mechanism of recognition is linked to the physical structure of the activator. In line with that hypothesis, our results have shown that the fibrillar state of A β was a requirement for IL-1 β release.

Furthermore, we found that phagocytosis of A β was necessary for that pathway. We found that once A β was phagocytosed by microglial cells, A β -containing lysosomes adopted a swollen morphology and underwent structural damage, as indicated by loss of their pH-lowering capacity. Other studies have reported that microglial cells are incapable of efficiently degrading fibrillar A β for a period of weeks after its internalization³⁰. This 'frustrated' degradation of A β may contribute to the loss of lysosomal integrity, which in turn triggers the release of lysosomal components into the cytoplasm, as noted here. The release of such factors seems to be causally involved in the initiation of the A β -induced IL-1 β pathway, as we found that IL-1 β release depended on the lysosomal protease cathepsin B.

Cathepsin B has already been linked to the pathogenesis of Alzheimer's disease. For example, larger amounts of cathepsin B have been reported in microglia surrounding senile plaques¹⁸, and pharmacological inhibition of cathepsin B delays memory loss and decreases the A β plaque burden in a mouse model of Alzheimer's disease¹⁹. So far, most studies have focused on the function of cathepsin B in the cleavage of amyloid precursor protein in neurons^{19,31} and the extracellular removal of A β from senile plaques¹⁸. Our study has suggested an additional effect of cathepsin B; that is, that cathepsin B serves as an intermediary among A β phagocytosis, lysosomal damage and microglial IL-1 β release. Notably, lysosomal leakage after A β internalization has also been noted in neuronal cultures³². However, in the cells surrounding senile plaques, NALP3 is expressed only by mononuclear phagocytes, not by neurons³³. It remains to be determined whether cathepsin B interacts directly with the inflammasome or whether this process involves intermediary molecules activated by cathepsin B. Our experiments have indicated that cathepsin B acts 'upstream' of NALP3 rather than influencing the production of pro-IL-1 or release of mature IL-1 β . Furthermore, as lysosomes contain many other components, other phagosomal factors, including other cathepsins, could additionally contribute to inflammasome activation.

Unexpectedly, we also found that the NALP3–caspase-1 pathway was pivotal in the A β -induced secretion of critical proinflammatory, chemotactic and potentially neurotoxic cytokines *in vitro*, including TNF and nitric oxide. The central importance of the inflammatory axis initiated by the NALP3–caspase-1 pathway and IL-1 was emphasized by our finding that activation and recruitment of microglia by exogenous fibrillar A β was much lower *in vivo* in mice deficient in ASC, caspase-1, IL-1R or MyD88. Similar to our results, other studies have reported that in human monocytes, the release of TNF and IL-6 triggered by urate crystals, another endogenous 'danger' signal, is regulated by the IL-1 β signaling pathway¹¹. This indicates that IL-1 signaling is essential or at least contributes to the production of various proinflammatory cytokines and chemokines. The receptors for IL-1 and IL-18 contain an intracellular signaling domain (Toll–IL-1R) that is shared by all Toll-like receptors³⁴. Thus, it is not unexpected that the 'downstream' signaling events from IL-1, such as the induction of proinflammatory cytokines, overlap those noted after activation of Toll-like receptors.

The recruitment and activation of invading macrophages and microglia to senile plaques is a critical and early step in the initiation and progression of neuronal dysfunction and eventual neuronal death². Furthermore, several of the microglial cytokines we have identified here as being regulated by the NALP3–caspase-1 pathway have been shown before to induce neuronal cell death *in vitro*^{21,22}. Other studies, however, have reported that microglial recruitment and activation may also have beneficial effects on plaque removal and disease progression, which indicates that the involvement of inflammatory responses in the pathogenesis of Alzheimer's disease *in vivo* is more complex^{3,27,35}. The issues of whether the pathways we have described here are actually beneficial or deleterious to the brain and to what extent they interact with other pathways, such as those activated by Toll-like receptors^{36,37} or scavenger receptors²⁵, must be addressed by future studies with transgenic mouse models of Alzheimer's disease. Our findings have suggested that pharmacological intervention aimed at this critical control point of microglial recruitment and activation may hold therapeutic promise. However, the complexity and interdependence on the cytokine network suggest that narrowly targeted anti-inflammatory therapy for patients with Alzheimer's disease, such as the use of caspase-1 inhibitors, may have unanticipated effects.

METHODS

Mice

NALP3-deficient mice (*Nlrp3*^{-/-})²⁸, ASC-deficient mice (*Pycard*^{-/-})²⁸ and IPAF-deficient mice (*Nlrp4*^{-/-})³⁸ were from Millennium Pharmaceuticals. MyD88-deficient mice (*Myd88*^{-/-}) and caspase-1-deficient mice (*Casp1*^{-/-})³⁹ were provided by S. Akira and A. Hise, respectively. Cathepsin B-deficient mice (*Ctsb*^{-/-}) have been described⁴⁰. C57BL/6 mice and IL-1R-deficient mice (*Il1r1*^{-/-}) were from Jackson Laboratories. All mouse strains were housed and bred in pathogen-free conditions. All experiments were in accordance with the guidelines set forth by the University of Massachusetts Medical School Department of Animal Medicine and approved by the Institutional Animal Care and Use Committee.

Reagents

ATP, cytochalasin D, LPS, pepstatin A (cathepsin D inhibitor), poly-L-lysine, BSA, poly(dA:dT) (poly(deoxyadenylic-thymidylic) acid, sodium salt), saponin and zymosan were from Sigma-Aldrich. Specific inhibitors of cathepsin B (CA-074-Me) and cathepsin L (Z-FF-fmk) were from Calbiochem. Goat anti-mouse cathepsin B (AF953) was from R&D Systems; mouse anti-mammalian neuronal class III β -tubulin (TUJ-1) was from Covance; rat anti-mouse CD11b (5C6) and rat anti-mouse F4/80 (MCA497R) were from Serotec; biotin-labeled rat anti-mouse CD107A (LAMP-1; 13-1071) was from eBioscience; and polyclonal rabbit anti-glial fibrillary acidic protein (Z0334) was from Dako. Alexa Fluor 647-conjugated goat anti-rabbit, Alexa Fluor 568-conjugated streptavidin, Alexa Fluor 488-conjugated goat anti-mouse, Alexa Fluor 568-conjugated donkey anti-goat, Alexa Fluor 647-conjugated and Alexa Fluor 488-conjugated goat anti-rat, Alexa Fluor 647-conjugated cholera toxin subunit B, LysoTracker green, LysoTracker red and Hoechst 33258 were from Invitrogen. Recombinant mouse interferon- γ was from BD Pharmingen. Paraformaldehyde was from Electron Microscopy Sciences. The caspase-1-specific inhibitor z-YVAD-fmk (benzyloxycarbonyl-Tyr-Val-Ala-Asn-fluoromethylketone) was from BioVision Research Products.

A β

A peptide of amino acids 1–42 of A β and the same peptide conjugated to the fluorescent dye HiLyte 488, as well as revA β (control nonfibrillary peptide with identical sequence in reverse order), were from Anaspec or American Peptide and were prepared as described⁴¹. A β preparations were tested for endotoxin with a limulus amoebocyte lysate assay

(Associates of Cape Cod) and were found to be below the limit of detection. FITC-labeled A β was prepared according to the manufacturer's instructions (Invitrogen). Unbound FITC was removed by dialysis overnight in cold PBS.

Cell culture

For primary cultures, bone marrow–derived macrophages and microglia were isolated as described^{42,43} and were cultured in DMEM supplemented with L-glutamine, ciprofloxacin (Cellgro) and 10% (vol/vol) FCS (Hyclone). Immortalized macrophage and microglial cell lines were generated with J2 recombinant retrovirus (carrying the v-myc and v-raf oncogenes)^{44,45}. For the induction of macrophage differentiation, primary bone marrow cells were incubated for 3–4 d in medium conditioned by L929 mouse fibroblasts. Cells were then infected with J2 recombinant retrovirus and were maintained in culture until cells were growing in the absence of conditioned medium. Similarly, primary mixed glial cultures were cultured until fully confluent. After two consecutive infections with J2 retrovirus, cells were maintained in normal medium until there was growth of microglial cells in colonies. Semiadherent colonies of microglial cells were washed off and were cultured in new flasks. Microglial and macrophage cell lines were tested extensively. Immortalized microglial cells showed 100% purity and morphology and surface marker expression highly similar to primary microglia (Supplementary Fig. 1a,b). Microglial cell lines from wild-type (C57BL/6) mice and mice in deficient caspase-1 or IL-1R as well as macrophage cell lines from wild-type (C57BL/6) mice and mice in deficient NALP3, IPAF or ASC were also generated and used for experiments.

Cells were stimulated in serum-free DMEM. Microglial cells and macrophages were primed with interferon- γ (100 U/ml; Griess assay, enzyme-linked immunosorbent assay (ELISA) of TNF and real-time quantitative PCR) or ultrapure LPS (100 ng/ml; ELISA of IL-1 β , assays with FAM-YVAD-fmk (fluorescence-labeled inhibitor of caspases; 5-carboxyfluorescein–Tyr-Val-Ala-Asp–fluoromethylketone), assay of the microglia cell line expressing CFP-ASC and immunoblot analysis) 1–3 h before stimulation with A β , revA β , zymosan or ATP or transfection with poly(dA:dT).

CFP-ASC–expressing microglia cell line

Human ASC was fused to CFP through the use of *Bgl*III and *Bam*HI in the plasmid pEF-BOS-CFP. Subsequently, CFP-ASC was cloned with *Xho*I and *Not*I into a modified form of the FUGW expression vector (FUGW-XN). FUGW-XN was modified by replacement of the GFP region with a new cutting site that created *Xho*I- and *Not*I-compatible ends after digestion with *Esp*3I.

Lentivirus was produced in human embryonic kidney (HEK293T) cells transfected with the FUGW-based expression vector encoding CFP-ASC, the lentiviral packaging plasmid pCMV-dR8.91 and envelope plasmid (VSV-G) with the TransIT-LT1 transfection reagent (Mirus Bio) as described⁴⁶. At 1 d after transfection, medium was replaced and, after 1 d more of culture, supernatants containing lentivirus were removed and filtered and were used to infect immortalized microglia cells.

For experiments, CFP-ASC–expressing microglial cells were seeded in duplicate in confocal dishes and stimulated. Alexa Fluor 647–labeled cholera toxin subunit B (dilution, 1:1,000) was added to stain cellular membranes. Cells were then imaged by confocal microscopy (Leica SP2 AOBs). Cells were fixed and five random fields were imaged in duplicate for quantification.

Neurotoxicity and caspase-1 assay

For assessment of microglia-induced neurotoxicity, CAD mouse neuronal cells⁴⁷ were seeded on poly-L-lysine-coated glass coverslips and were grown for 24 h in F12-DMEM supplemented with ciprofloxacin (Cellgro) and 10% (vol/vol) FCS (Hyclone). Differentiation was induced by withdrawal of serum for 48 h. Immortalized microglia from wild-type or caspase-1-deficient mice were added in serum-free medium to produce mixed neuronal-microglial cultures; these were immediately stimulated. At 72 h after stimulation with A β or media, cells were fixed, were stained for the neuron-specific marker TuJ-1 and the microglial marker CD11b and were imaged by confocal microscopy (Leica SP2 AOBS). Caspase-1 activity in microglial cells was assessed with a Caspase 1 FLICA kit (Immunochemistry Technologies) according to the manufacturer's instructions.

ELISA and nitric oxide measurement

Cell culture supernatants were assayed for IL-1 β and TNF with ELISA kits from R&D Systems according to the manufacturer's instructions. Nitric oxide was measured by the Griess reaction of nitrites accumulated in the supernatants with chemicals from Sigma.

Immunocytochemistry

Neuronal, microglial, mixed neuronal-microglial and primary mixed glial cultures were fixed for 30 min with 4% (vol/vol) paraformaldehyde, followed by incubation for 2 h at 25 °C with the appropriate primary and secondary antibodies in PBS containing 1% (wt/vol) BSA, 5% (vol/vol) FCS and 0.05% (vol/vol) saponin. Cell nuclei were stained with Hoechst 33258 (dilution, 1:1,000).

Stereotaxic brain microinjection

Brains were injected as described²⁷. Six-week-old mice ($n = 4$ per group) were anesthetized with ketamine (100 mg per kg body weight, given intraperitoneally; Webster) and xylazine (10 mg per kg body weight, given intraperitoneally; Webster), then were placed on a homeothermic heating blanket (Harvard Apparatus) and immobilized in a stereotaxic frame (Stoelting). A linear skin incision was made in sterile conditions and a small hole was created in the skull with a dental drill 1 mm anterior and 2 mm lateral to bregma over both hemispheres. The left side was inoculated with 1 μ l A β in sterile pyrogen-free saline (1 mg/ml) and the right side was inoculated with the same amount of revA β , with separate Hamilton syringes. Mice were allowed to fully recover on a heating blanket. After 48 h, mice were anesthetized with ketamine-xylazine and were transcardially perfused with 4% (vol/vol) paraformaldehyde in PBS. Brains were removed and were placed overnight at 4 °C in 4% (vol/vol) paraformaldehyde, then were transferred to PBS and were stored at 4 °C until they were sectioned. Coronal sections 60 μ m in thickness were made with a Vibratome (Leica). Antigens were retrieved by incubation of the slices for 6 min in protease K (Invitrogen) at a concentration of 20 μ g/ml in Tris-EDTA buffer, pH 8.0. Slices were blocked for 1 h in PBS containing 0.3% (vol/vol) Triton X-100 (Fisher), 10% (vol/vol) horse serum and 1% (vol/vol) BSA and then were incubated for 24 h at 25 °C with primary antibody (rat anti-F4/80; dilution, 1:100; MCA497R; Serotec) in 5% (vol/vol) horse serum and 0.05% (vol/vol) Triton X-100 in PBS. Staining was visualized by incubation for 3 h at 25 °C with Alexa Fluor 488-conjugated secondary antibody (goat anti-rat; dilution, 1:500; Invitrogen). Cell nuclei were stained with Hoechst 33258 (dilution, 1:1,000). Images were obtained with a confocal microscope (Zeiss). For quantification of microglia recruited to sites of microinjection, serial sections from each site of injection were visualized by fluorescence microscopy (Nikon Eclipse E400) and were digitally photographed. Microscope settings were the same for all experiments. The fluorescence intensity of

microglia immunoreactive for F4/80 at each injection site was quantified with ImageJ (NIH).

Flow cytometry

For evaluation of lysosomal damage, cells were incubated for 30 min with LysoTracker green (dilution, 1:2000) and then were stimulated. Lysosomal damage was defined as loss of LysoTracker fluorescence, as assessed by flow cytometry. An LSRII cytometer (BD Biosciences) was used for all flow cytometry; data were acquired with DIVA software (BD Biosciences) and analyzed with FlowJo software (Tree Star).

Quantitative real-time PCR

Immortalized mouse microglia were seeded in six-well tissue culture plates, were incubated in the absence or presence of 10 μ M A β , were washed with PBS and were lysed in 1 ml TRIzol reagent (Invitrogen). RNA was purified by organic extraction. RNA (5 μ g from each sample) was reverse-transcribed with MultiScribe reverse transcriptase (Applied Biosystems). Oligonucleotide primers were designed with the Primer3 Input PCR primer-design program (version 0.4.0.), and the iQ Real-Time PCR Detection system (Bio-Rad) and Optical System Software (Version 2.0, Bio-Rad) were used for quantitative real-time PCR. Quantification of mRNA expression relative to that in unstimulated conditions was calculated by the comparative cycle method as described by the manufacturer.

Immunoblot analysis

Cell culture supernatants were precipitated by the addition of an equal volume of methanol and 0.25 volumes of chloroform, followed by vortexing and centrifugation for 10 min at 20,000g. The upper phase was discarded and 500 μ l methanol was added to the interphase. This mixture was centrifuged at for 10 min at 20,000g and the protein pellet was dried at 55 $^{\circ}$ C, resuspended in Laemmli buffer and boiled for 5 min at 99 $^{\circ}$ C. Samples were separated by SDS-PAGE (15%) and were transferred onto nitrocellulose membranes. Blots were incubated with rabbit polyclonal anti-mouse caspase-1 p10 (sc-514; Santa Cruz Biotechnology).

Supplementary Material

Refer to Web version on PubMed Central for supplementary material.

Acknowledgments

MyD88-deficient mice were provided by S. Akira (University of Osaka) and caspase-1-deficient mice were provided by A. Hise (Case Western Reserve University). We thank A. Cerny and J. Boulanger for animal husbandry and care, and K. Wozniak and S. Zhou for advice. Supported by the German Academic Exchange Office (A.H.), a European Union Marie Curie Fellowship (G.C.P.), the German Science Foundation (V.H.) and the US National Institutes of Health (GM54060 and AI065483 to D.T.G. and E.L.; AG20255 to K.J.M.).

References

1. Weiner HL, Frenkel D. Immunology and immunotherapy of Alzheimer's disease. *Nat. Rev. Immunol.* 2006; 6:404–416. [PubMed: 16639431]
2. Meyer-Luehmann M, et al. Rapid appearance and local toxicity of amyloid- β plaques in a mouse model of Alzheimer's disease. *Nature.* 2008; 451:720–724. [PubMed: 18256671]
3. Simard AR, Soulet D, Gowing G, Julien JP, Rivest S. Bone marrow-derived microglia play a critical role in restricting senile plaque formation in Alzheimer's disease. *Neuron.* 2006; 49:489–502. [PubMed: 16476660]

4. Itagaki S, McGeer PL, Akiyama H, Zhu S, Selkoe D. Relationship of microglia and astrocytes to amyloid deposits of Alzheimer disease. *J. Neuroimmunol.* 1989; 24:173–182. [PubMed: 2808689]
5. Weggen S, et al. A subset of NSAIDs lower amyloidogenic A β 42 independently of cyclooxygenase activity. *Nature.* 2001; 414:212–216. [PubMed: 11700559]
6. Schenk D, et al. Immunization with amyloid- β attenuates Alzheimer-disease-like pathology in the PDAPP mouse. *Nature.* 1999; 400:173–177. [PubMed: 10408445]
7. Akama KT, Van Eldik LJ. β -amyloid stimulation of inducible nitric-oxide synthase in astrocytes is interleukin-1 β - and tumor necrosis factor- α (TNF α)-dependent, and involves a TNF α receptor-associated factor- and NF κ B-inducing kinase-dependent signaling mechanism. *J. Biol. Chem.* 2000; 275:7918–7924. [PubMed: 10713108]
8. Griffin WS, et al. Brain interleukin 1 and S-100 immunoreactivity are elevated in Down syndrome and Alzheimer disease. *Proc. Natl. Acad. Sci. USA.* 1989; 86:7611–7615. [PubMed: 2529544]
9. Blum-Degen D, et al. Interleukin-1 β and interleukin-6 are elevated in the cerebrospinal fluid of Alzheimer's and de novo Parkinson's disease patients. *Neurosci. Lett.* 1995; 202:17–20. [PubMed: 8787820]
10. Dinarello CA. A signal for the caspase-1 inflammasome free of TLR. *Immunity.* 2007; 26:383–385. [PubMed: 17459804]
11. Martinon F, Petrilli V, Mayor A, Tardivel A, Tschopp J. Gout-associated uric acid crystals activate the NALP3 inflammasome. *Nature.* 2006; 440:237–241. [PubMed: 16407889]
12. Mariathasan S, et al. Cryopyrin activates the inflammasome in response to toxins and ATP. *Nature.* 2006; 440:228–232. [PubMed: 16407890]
13. Dostert C, et al. Innate immune activation through Nalp3 inflammasome sensing of asbestos and silica. *Science.* 2008; 320:674–677. [PubMed: 18403674]
14. Amstad PA, et al. Detection of caspase activation in situ by fluorochrome-labeled caspase inhibitors. *Biotechniques.* 2001; 31:608–610. [PubMed: 11570504]
15. Agostini L, et al. NALP3 forms an IL-1 β -processing inflammasome with increased activity in Muckle-Wells autoinflammatory disorder. *Immunity.* 2004; 20:319–325. [PubMed: 15030775]
16. Fernandes-Alnemri T, et al. The pyroptosome: a supramolecular assembly of ASC dimers mediating inflammatory cell death via caspase-1 activation. *Cell Death Differ.* 2007; 14:1590–1604. [PubMed: 17599095]
17. Liu Y, et al. LPS receptor (CD14): a receptor for phagocytosis of Alzheimer's amyloid peptide. *Brain.* 2005; 128:1778–1789. [PubMed: 15857927]
18. Mueller-Stieber S, et al. Anti-amyloidogenic and neuroprotective functions of cathepsin B: implications for Alzheimer's disease. *Neuron.* 2006; 51:703–714. [PubMed: 16982417]
19. Hook VY, Kindy M, Hook G. Inhibitors of cathepsin B improve memory and reduce β -amyloid in transgenic Alzheimer disease mice expressing the wild-type, but not the Swedish mutant, β -secretase site of the amyloid precursor protein. *J. Biol. Chem.* 2008; 283:7745–7753. [PubMed: 18184658]
20. Buttle DJ, Murata M, Knight CG, Barrett AJ. CA074 methyl ester: a proinhibitor for intracellular cathepsin B. *Arch. Biochem. Biophys.* 1992; 299:377–380. [PubMed: 1444478]
21. Xie Z, et al. Peroxynitrite mediates neurotoxicity of amyloid β -peptide1–42- and lipopolysaccharide-activated microglia. *J. Neurosci.* 2002; 22:3484–3492. [PubMed: 11978825]
22. Combs CK, Karlo JC, Kao SC, Landreth GE. β -Amyloid stimulation of microglia and monocytes results in TNF α -dependent expression of inducible nitric oxide synthase and neuronal apoptosis. *J. Neurosci.* 2001; 21:1179–1188. [PubMed: 11160388]
23. Mariathasan S, Monack DM. Inflammasome adaptors and sensors: intracellular regulators of infection and inflammation. *Nat. Rev. Immunol.* 2007; 7:31–40. [PubMed: 17186029]
24. Li M, Pisalyaput K, Galvan M, Tenner AJ. Macrophage colony stimulatory factor and interferon- γ trigger distinct mechanisms for augmentation of β -amyloid-induced microglia-mediated neurotoxicity. *J. Neurochem.* 2004; 91:623–633. [PubMed: 15485493]
25. El Khoury JB, et al. CD36 mediates the innate host response to β -amyloid. *J. Exp. Med.* 2003; 197:1657–1666. [PubMed: 12796468]

26. Weldon DT, et al. Fibrillar β -amyloid induces microglial phagocytosis, expression of inducible nitric oxide synthase, and loss of a select population of neurons in the rat CNS in vivo. *J. Neurosci.* 1998; 18:2161–2173. [PubMed: 9482801]
27. El Khoury J, et al. *Ccr2* deficiency impairs microglial accumulation and accelerates progression of Alzheimer-like disease. *Nat. Med.* 2007; 13:432–438. [PubMed: 17351623]
28. Kanneganti TD, et al. Bacterial RNA and small antiviral compounds activate caspase-1 through cryopyrin/Nalp3. *Nature.* 2006; 440:233–236. [PubMed: 16407888]
29. Ishii KJ, Coban C, Akira S. Manifold mechanisms of Toll-like receptor-ligand recognition. *J. Clin. Immunol.* 2005; 25:511–521. [PubMed: 16380815]
30. Frackowiak J, et al. Ultrastructure of the microglia that phagocytose amyloid and the microglia that produce β -amyloid fibrils. *Acta Neuropathol.* 1992; 84:225–233. [PubMed: 1414275]
31. Cataldo AM, Barnett JL, Pieroni C, Nixon RA. Increased neuronal endocytosis and protease delivery to early endosomes in sporadic Alzheimer's disease: neuropathologic evidence for a mechanism of increased β -amyloidogenesis. *J. Neurosci.* 1997; 17:6142–6151. [PubMed: 9236226]
32. Yang AJ, Chandswangbhuvana D, Margol L, Glabe CG. Loss of endosomal/lysosomal membrane impermeability is an early event in amyloid $A\beta$ 1–42 pathogenesis. *J. Neurosci. Res.* 1998; 52:691–698. [PubMed: 9669318]
33. Kummer JA, et al. Inflammasome components NALP 1 and 3 show distinct but separate expression profiles in human tissues suggesting a site-specific role in the inflammatory response. *J. Histochem. Cytochem.* 2007; 55:443–452. [PubMed: 17164409]
34. Boraschi D, Tagliabue A. The interleukin-1 receptor family. *Vitam. Horm.* 2006; 74:229–254. [PubMed: 17027517]
35. Shafiq SS, et al. Sustained hippocampal IL-1 β overexpression mediates chronic neuroinflammation and ameliorates Alzheimer plaque pathology. *J. Clin. Invest.* 2007; 117:1595–1604. [PubMed: 17549256]
36. Richard KL, Filali M, Prefontaine P, Rivest S. Toll-like receptor 2 acts as a natural innate immune receptor to clear amyloid β 1–42 and delay the cognitive decline in a mouse model of Alzheimer's disease. *J. Neurosci.* 2008; 28:5784–5793. [PubMed: 18509040]
37. Tahara K, et al. Role of toll-like receptor signalling in $A\beta$ uptake and clearance. *Brain.* 2006; 129:3006–3019. [PubMed: 16984903]
38. Franchi L, et al. Cytosolic flagellin requires Ipaf for activation of caspase-1 and interleukin 1 β in salmonella-infected macrophages. *Nat. Immunol.* 2006; 7:576–582. [PubMed: 16648852]
39. Kuida K, et al. Altered cytokine export and apoptosis in mice deficient in interleukin-1 β converting enzyme. *Science.* 1995; 267:2000–2003. [PubMed: 7535475]
40. Halangk W, et al. Role of cathepsin B in intracellular trypsinogen activation and the onset of acute pancreatitis. *J. Clin. Invest.* 2000; 106:773–781. [PubMed: 10995788]
41. Moore KJ, et al. A CD36-initiated signaling cascade mediates inflammatory effects of β -amyloid. *J. Biol. Chem.* 2002; 277:47373–47379. [PubMed: 12239221]
42. Severa M, Coccia EM, Fitzgerald KA. Toll-like receptor-dependent and -independent viperin gene expression and counter-regulation by PRDI-binding factor-1/BLIMP1. *J. Biol. Chem.* 2006; 281:26188–26195. [PubMed: 16849320]
43. Lehnardt S, et al. A mechanism for neurodegeneration induced by group B streptococci through activation of the TLR2/MyD88 pathway in microglia. *J. Immunol.* 2006; 177:583–592. [PubMed: 16785556]
44. Roberson SM, Walker WS. immortalization of cloned mouse splenic macrophages with a retrovirus containing the *v-raf/mil* and *v-myc* oncogenes. *Cell. Immunol.* 1988; 116:341–351. [PubMed: 2460250]
45. Blasi E, Barluzzi R, Bocchini V, Mazzolla R, Bistoni F. immortalization of murine microglial cells by a *v-raf/v-myc* carrying retrovirus. *J. Neuroimmunol.* 1990; 27:229–237. [PubMed: 2110186]
46. Lois C, Hong EJ, Pease S, Brown EJ, Baltimore D. Germline transmission and tissue-specific expression of transgenes delivered by lentiviral vectors. *Science.* 2002; 295:868–872. [PubMed: 11786607]

47. Qi Y, Wang JK, McMillian M, Chikaraishi DM. Characterization of a CNS cell line, CAD, in which morphological differentiation is initiated by serum deprivation. *J. Neurosci.* 1997; 17:1217–1225. [PubMed: 9006967]

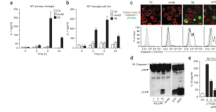
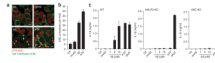


Figure 1.

Fibrillar A β induces the caspase-1-dependent release of interleukin-1 β . **(a,b)** ELISA of the release of IL-1 β by wild-type (WT) primary mouse microglia **(a)** and immortalized mouse microglia **(b)** left untreated (Ctl) or stimulated with fibrillar A β (10 μ M) or revA β (10 μ M). **(c)** Confocal microscopy (above) and flow cytometry (below) of activated caspase-1 (green) in wild-type immortalized microglial cells left untreated or incubated for 4 h with A β (10 μ M), revA β (10 μ M) or ATP (1 mM); caspase-1 activation was visualized by incubation with a fluorescent cell-permeable probe that binds only to activated caspase-1 (FLICA), and cell membranes were stained for cholera toxin subunit B (red). Scale bar, 10 μ m. Gray filled histograms, unstimulated control cells. **(d)** Immunoblot analysis of caspase-1 (p10) cleavage in LPS-primed wild-type bone marrow-derived macrophages stimulated with A β (1, 5 and 10 μ M), revA β (10 μ M) or ATP (5 mM) or transfected with poly(dA:dT) (dAdT; 1.6 μ g). p45, full-length pro-form of caspase-1. **(e)** ELISA of the release of IL-1 β into supernatants of wild-type immortalized microglial cells left unstimulated or stimulated for 6 h with A β in the presence of increasing amounts of a caspase-1-specific inhibitor (z-YVAD-fmk). Data are representative of experiments done three times (error bars **(a,b,e)**, s.e.m.).

**Figure 2.**

Fibrillar A β activates the NALP3 inflammasome. **(a)** Confocal microscopy of wild-type immortalized microglial cells stably transduced with CFP-ASC, left unstimulated or stimulated for 4 h with revA β (10 μ M), A β (10 μ M) or ATP (1 mM) in duplicate after being primed with LPS; cell membranes were stained with fluorescent cholera toxin subunit B (Ctb; green), and arrowheads indicate clusters of CFP-ASC (red). Scale bars, 10 μ m. **(b)** Quantification of the images in **a** (mean and s.e.m. of five random fields). Data are representative of experiments done twice with nearly identical results. **(c)** ELISA of the release of IL-1 β into the supernatants of LPS-primed bone marrow-derived wild-type, NALP3-deficient (NALP3-KO) and ASC-deficient (ASC-KO) macrophages left unstimulated or stimulated with A β (1, 5 or 10 μ M), revA β (10 μ M) or ATP (5 mM) or transfected with poly(dA:dT) (200 ng) for 6 h. Data are representative of experiments done twice (error bars, s.e.m.).

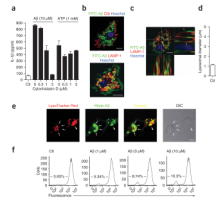
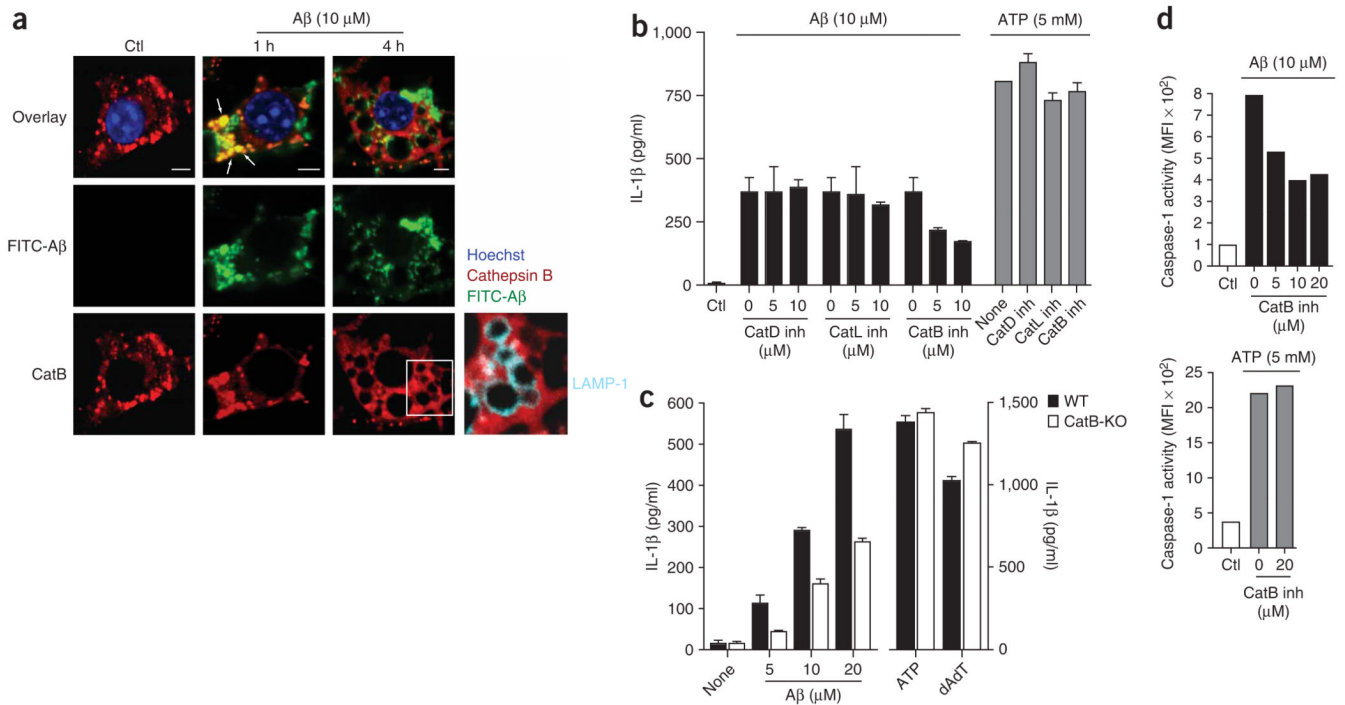
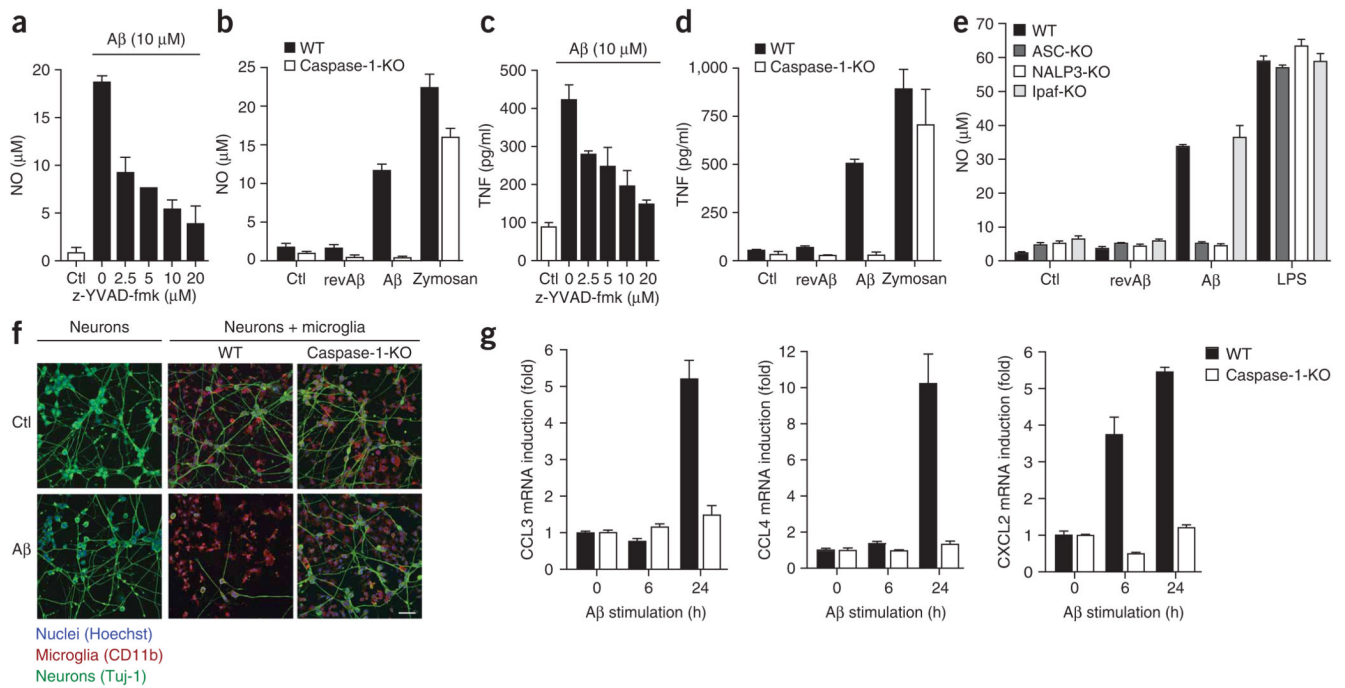


Figure 3.

Phagocytosis of A β is necessary for IL-1 β release and induces lysosomal damage. **(a)** ELISA of the release of IL-1 β into supernatants of wild-type immortalized microglia treated with cytochalasin D during stimulation with A β or ATP. **(b,c)** Confocal microscopy of immortalized microglia incubated for 4 h with FITC-labeled A β (10 μ M) and then processed for immunocytochemistry; cell membranes were visualized with cholera toxin subunit B and lysosomes were stained with anti-LAMP-1. Arrows indicate LAMP-1-positive lysosomes containing A β ; z-series (top right and bottom left, **c**) were taken through the dashed lines (top left, **c**). Scale bars, 10 μ m. **(d)** Lysosomal diameter in unstimulated cells (Ctl) and cells that incorporated A β ($n = 50$ cells per group). **(e)** Confocal microscopy of lysosomal integrity in wild-type microglia incubated with acidophilic lysomotropic dye (LysoTracker Red; red), and then stimulated with HiLyte 488-conjugated A β (green). Arrowheads indicate phagocytosed A β overlaid with the lysomotropic dye in small lysosomes; arrows indicate enlarged A β -containing dye-negative lysosomes, indicative of perturbation of lysosomal integrity. Scale bar, 10 μ m. **(f)** Quantification of the loss of fluorescence in **e** by flow cytometry of wild-type microglia left untreated or treated with A β (1, 3 or 10 μ M). Numbers in plots indicate percent cells negative for fluorescence. Data are representative of experiments done three times with similar results (error bars (**a,d**), s.e.m.).

**Figure 4.**

Lysosomal damage triggers the release of cathepsin B, which is involved in the IL-1 β pathway. **(a)** Confocal microscopy of microglial cells left unstimulated or stimulated for 1 or 4 h with FITC-labeled A β (green), and then stained with anti-cathepsin B (red) or anti-LAMP-1 (cyan; far right); nuclei were stained with Hoechst 33258 (blue). Arrows indicate colocalization of cathepsin B and A β . Scale bars, 5 μ m. **(b)** Effect of various concentrations (0, 5 or 10 μ M) of inhibitors of cathepsin D (CathD inh), cathepsin L (CathL inh) or cathepsin B (CathB inh) on the A β -induced release of IL-1 β from LPS-primed immortalized microglia (left) and the effect of cathepsin inhibitors at the highest concentration (10 μ M) on IL-1 β release induced by ATP (right). **(c)** ELISA of the release of IL-1 β by wild-type and cathepsin B-deficient primary macrophages left unstimulated or after stimulation with A β , ATP or poly(dA:dT). **(d)** Caspase-1 activation in microglial cells after stimulation with A β (above) or ATP (below) and treatment with the cathepsin B inhibitor (20 μ M), assessed by flow cytometry with a fluorescent cell-permeable probe that binds only to activated caspase-1. MFI, mean fluorescence intensity. Data are representative of two **(a,c)** or three **(b,d)** separate experiments (error bars **(b-d)**, s.e.m.).

**Figure 5.**

A β -induced expression of proinflammatory and chemotactic factors is mediated by caspase-1 activation in microglia. **(a)** A β -induced production of nitric oxide (NO) by immortalized microglia after 1 h of pretreatment with the caspase-1-specific inhibitor z-YVAD-fmk. **(b)** Production of nitric oxide by immortalized wild-type and caspase-1-deficient cells after stimulation for 24 h with A β , revA β or zymosan (10 μ g/ml) or without stimulation. **(c,d)** ELISA of TNF production by the cells in **a** (**c**) or **b** (**d**). **(e)** Production of nitric oxide by immortalized wild-type, ASC-, NALP3- or Ipaf-deficient macrophages left unstimulated or stimulated for 24 h with revA β (10 μ M), A β (10 μ M) or LPS (100 ng/ml). **(f)** Confocal microscopy of CAD mouse neuronal cells cultured with microglia from wild-type and caspase-1-deficient mice, then stimulated with A β (10 μ M, 72 h), and then fixed and stained with antibodies specific for neurons (TUJ-1; green) and microglia (CD11b; red); nuclei were stained with Hoechst 33258 (blue). Scale bar, 50 μ m. **(g)** Real-time quantitative PCR of CCL3, CCL4 and CXCL2 mRNA in primed, immortalized wild-type and caspase-1-deficient microglia stimulated for 0, 6 or 24 h with A β , presented as 'fold induction' relative to that of unstimulated cells. Data are representative of experiments done three times with nearly identical results (**a–e**), experiments done twice (**f**) or experiments done three times (**g**; error bars (**a–e,g**), s.e.m.).

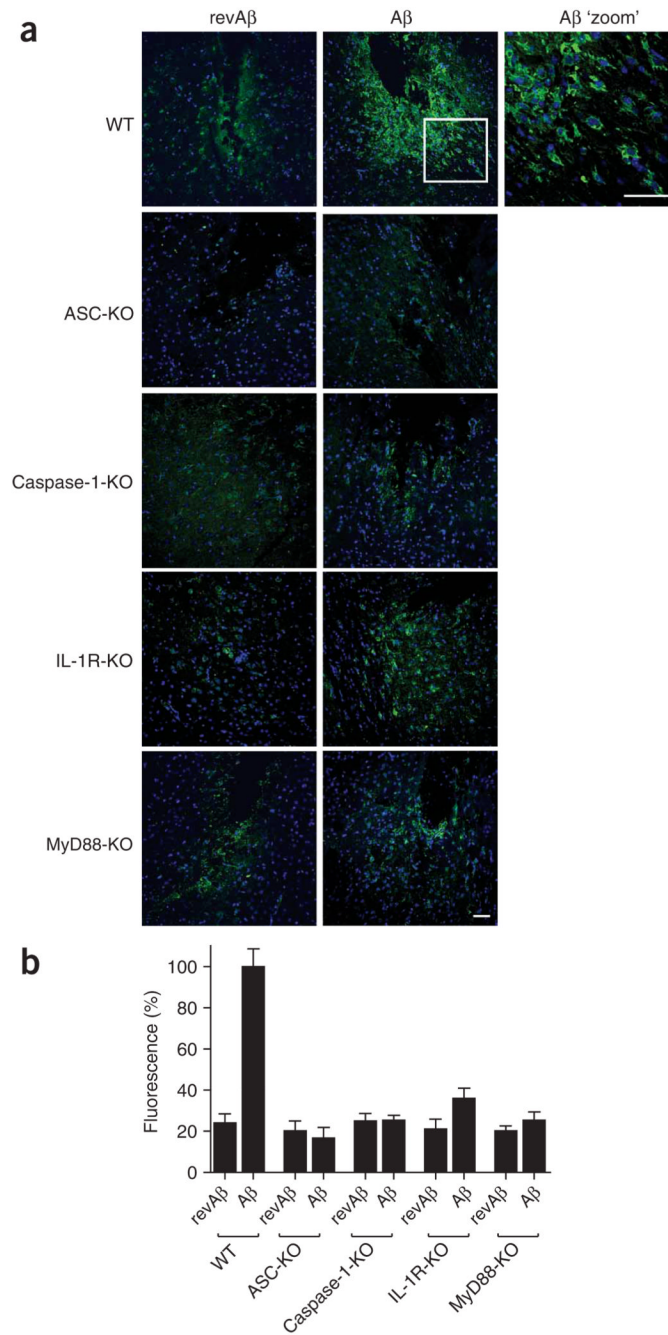


Figure 6.

IL-1-mediated pathways contribute to microglial activation induced by A β *in vivo*. **(a)** Confocal microscopy of coronal brain sections from wild-type mice and mice deficient in ASC, caspase-1, IL-1R or MyD88 at 48 h after stereotactical microinjection of A β (1 μ g) into the striatum and revA β into the contralateral hemisphere (control); sections are stained with anti-F4/80 (green) and nuclei are stained with Hoechst 33258 (blue). Scale bars, 50 μ m. **(b)** Quantification of the fluorescence intensity of the F4/80 staining in **a** to assess recruited microglia and mononuclear phagocytes, normalized to that of wild-type mice treated with A β (set as 100%) and presented as the mean and s.e.m. of each group ($n = 4$ mice per group,

with five consecutive sections quantified for each mouse). Data are representative of experiments done twice with each mouse.